Figures and figure supplements

NG2 glia are required for vessel network formation during embryonic development

Shilpi Minocha *et al*

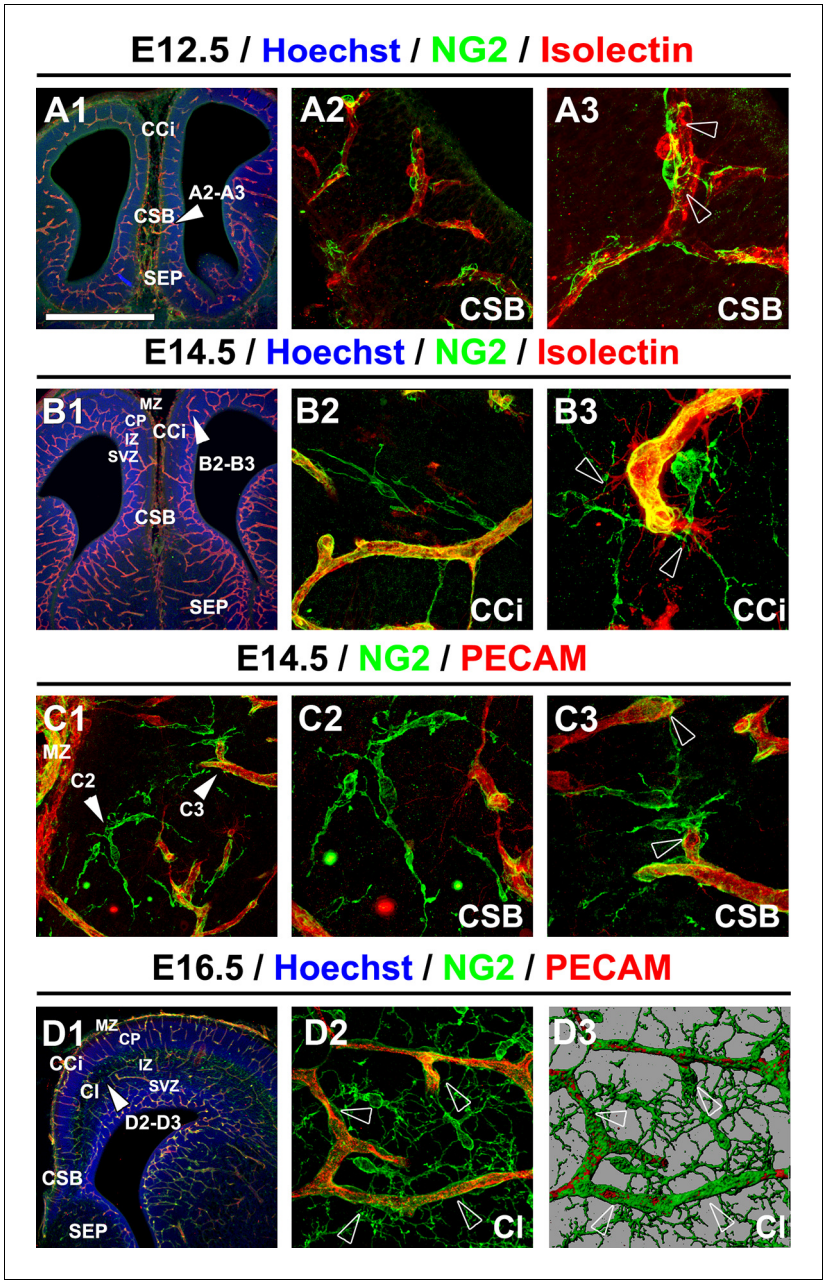

Figure 1. NG2^{+} glia are in close contact with blood vessels. (**A–D**) Double immunohistochemistry for NG2 and Isolectin (**A1–A3, B1–B3**) and for NG2 and PECAM (**C1–C3, D1–D2**) on coronal cingulate cortex (CCi) and cingulate bundle (CI) sections of wild-type mice (n=3 each) at E12.5 (**A1–A3**), at E14.5 (**B1–B3** and **C1–C3**), and at E16.5 (**D1–D2**). **A3, A2, B2, B3, C2, C3**,and **D2** are higher power views of the region in **A1, B1, C1,** and **D1**, respectively (white arrowheads). **D3** is an isosurface reconstruction of the labeling seen in **D2**. The processes of the NG2^{+} glia are in close contact with adjacent blood vessels (open arrowheads in **A3, B3,** and **C3**). Bar = 675 μm in **A1, B1,** and **D1**; 50 μm in **A2, B2, C1,** and **D2**; 40 μm in **A3, B3, C2,** and **C3**. **CSB**, corticoseptal boundary at the midline where the corpus callosum will form.

DOI: 10.7554/eLife.09102.003

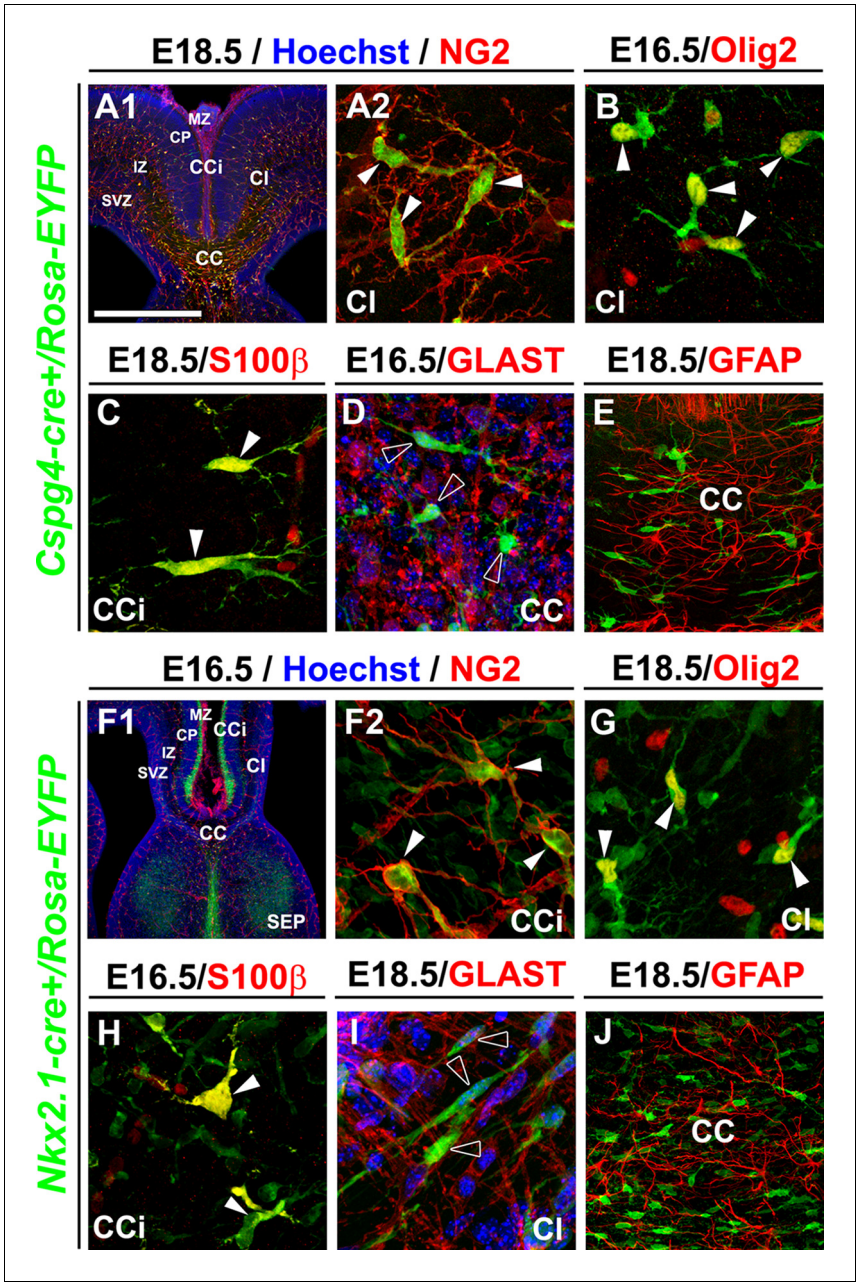

Figure 2. NG2$^+$ glia of the dorsal telencephalon are derived from Nkx2.1$^+$ progenitors of the subpallium. (**A–E**) Double immunohistochemistry for the YFP and NG2 (**A1–A2**) (n=3), the YFP and Olig2 (**B**) (n=3), the YFP and S100β (**C**) (n=3), the YFP and GLAST (**D**) (n=3), and the YFP and GFAP (**E**) (n=3) on telencephalic coronal slices of *Cspg4-cre*$^+$*/Rosa-EYFP* mice at E16.5 (**B** and **D**) and E18.5 (**A1, A2, C,** and **E**). (**F–J**) Double immunohistochemistry for the YFP and NG2 (**F1–F2**) (n=5), the YFP and Olig2 (**G**) (n=5), the YFP and S100β (**H**) (n=4), the YFP and GLAST (**I**) (n=4), and the YFP and GFAP (**J**) (n=3) on telencephalic coronal slices of *Nkx2.1-cre*$^+$*/Rosa-EYFP* mice at E16.5 (**F1, F2,** and **H**) and E18.5 (**G, I,** and **J**). **A2** and **F2** are higher power views of the cingulate region in **A1** and **F1**, respectively. The *NG2*-derived and the *Nkx2.1*-derived YFP$^+$ cells co-express polydendroglial markers, NG2 and Olig2, together with S100β (white arrowheads) but lack expression of GLAST and GFAP (open arrowheads in **D** and **I**). Bar=675 μm in **A1, F1**; 100 μm in **E, J**; 50 μm in **A2, B, C, D, F2, G, H, I**.

DOI: 10.7554/eLife.09102.004

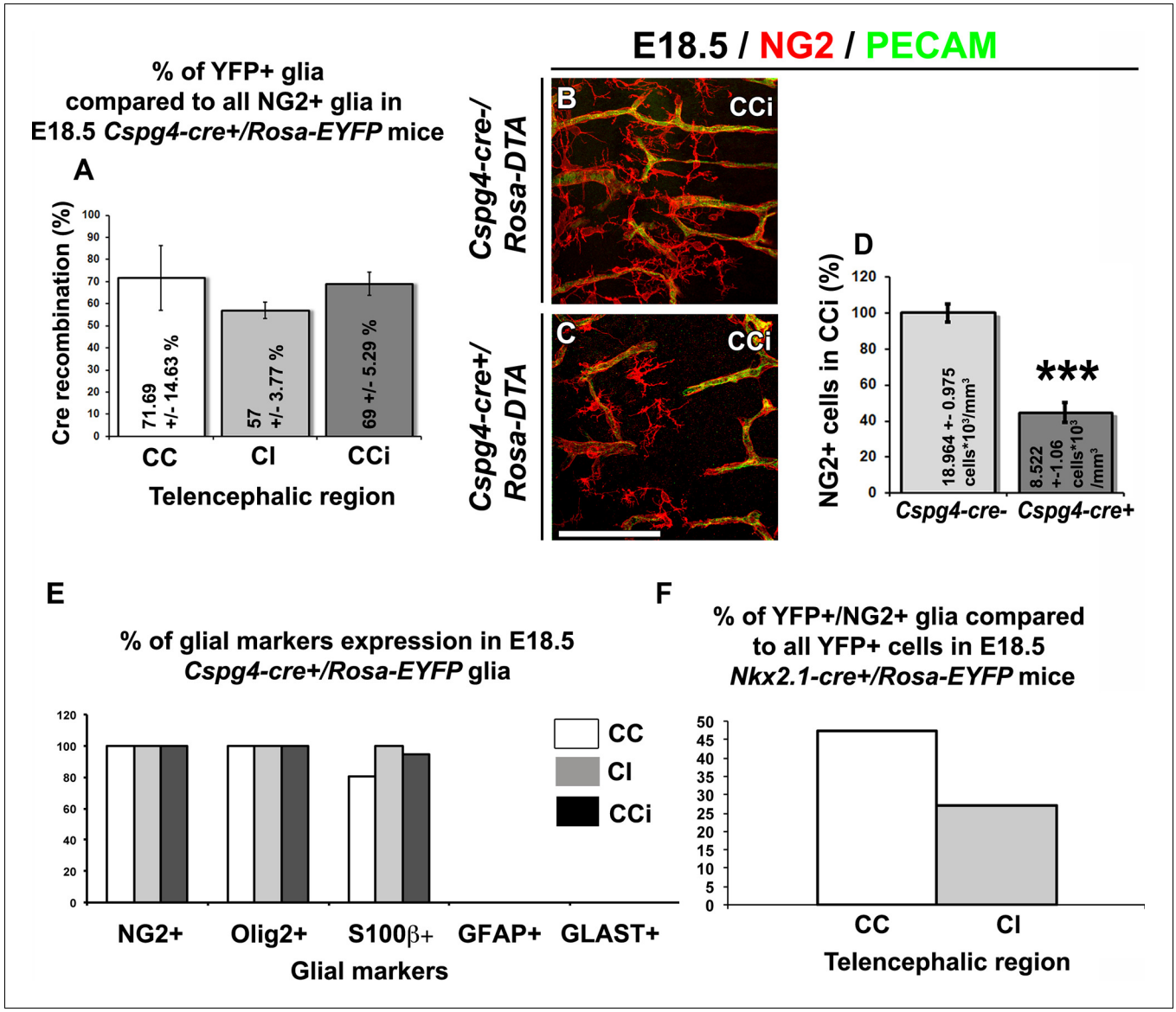

Figure 2—figure supplement 1. YFP signal in *Nkx2.1-cre*$^{+}$*/Rosa-EYFP* and *Cspg4-cre*$^{+}$*/Rosa-EYFP* mice is present in NG2 glia. (**A**) Bars (means ± SEM) represent the percentage of YFP-labeled NG2 glia in corpus callosum (CC), cingulate bundle (CI), and cingulate cortex (CCi) sections of E18.5 *Cspg4-cre*$^{+}$*/Rosa-EYFP* mice (n=3). The YFP signal in *Cspg4-cre*$^{+}$*/Rosa-EYFP* mice was detected in a majority of NG2^{+} embryonic glia of the dorsal telencephalon (71.7 ± 14.6% in the CC, 57 ± 3.8% in the CI and 69 ± 5.3% in the CCi at E16.5, n=3). (**B–C**) Double immunohistochemistry for NG2 and PECAM in CCi coronal sections of *Cspg4-cre*$^{-}$*/Rosa-DTA* (n=3) (**B**) and *Cspg4-cre*$^{+}$*/Rosa-DTA* (n=3) (**C**) mutant mice at E18.5. Scale bar = 50 μm in **B** and **C**. (**D**) Bars (means ± SEM; unpaired Student's *t*-test) represent the percentage of remaining NG2 glia in the telencephalon of E18.5 *Cspg4-cre*$^{+}$*/Rosa-DTA* mice compared to control mice. A drastic loss of NG2^{+} glia followed by severe vascular defects was observed in *Cspg4-cre*$^{+}$*/Rosa-DTA* mice compared to *Cspg4-cre*$^{-}$*/Rosa-DTA*. (**E**) Bars (means) represent the percentage of glial markers expression by YFP-labeled NG2 glia in the CC, CI, and CCi of E18.5 *Cspg4-cre*$^{+}$*/Rosa-EYFP* mice. In *Cspg4-cre*$^{+}$*/Rosa-EYFP* mice, all YFP-labeled NG2 glia of the dorsal telencephalon expressed NG2^{+}/Olig2^{+} (n=2), many S100β^{+} (n=2) but no GLAST^{+} (n=3) or GFAP^{+} (n=2). (**F**) Bars (means)represent the percentage of NG2 markers expression by YFP-labeled cells in the telencephalon of E18.5 *Nkx2.1-cre*$^{+}$*/Rosa-EYFP* mice (n=4) (47.24% in the CC and 27.2% in the CI). CC, corpus callosum; CCi, cingulate cortex; CI, cingulate bundle.

DOI: 10.7554/eLife.09102.005

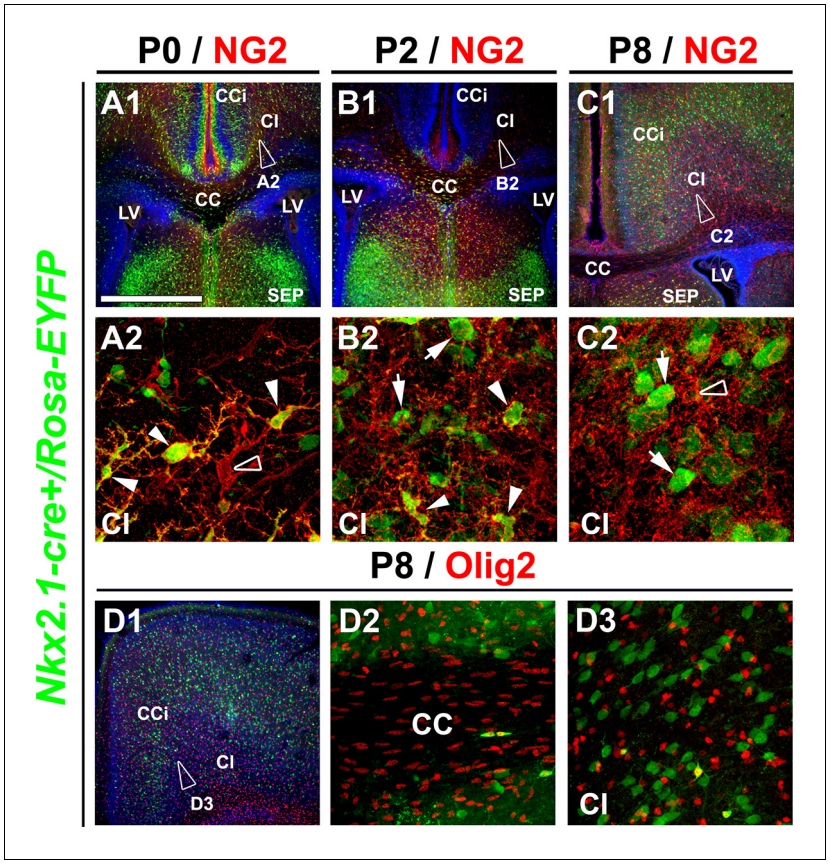

Figure 2—figure supplement 2. *Nkx2.1*-derived NG2 and Olig2 glia are transient and gradually disappear from the dorsal pallium at postnatal ages. (**A–C**) Double immunohistochemistry for GFP and NG2 on coronal telencephalicsections from *Nkx2.1-cre*$^{+}$*/Rosa-EYFP* mice at P0 (n=3) (**A1–A2**), P2 (n=3) (**B1–B2**), and P8 (n=2) (**C1–C2**). (**D**) Double immunohistochemistry for GFP and Olig2 on coronal telencephalicsections from *Nkx2.1-cre*$^{+}$*/Rosa-EYFP* mice at P8 (n=2) (**D1–D3**). Cell nuclei were counterstained in blue with Hoechst (**A1, B1,** and **C1**). **A2, B2, C2,** and **D3** are high-power views of the cingulate bundle (CI) seen in **A1, B1, C1**, and **D1**, respectively. In the CI of *Nkx2.1-cre*$^{+}$*/Rosa-EYFP* mice brains at P2, only very few *Nkx2.1*-derived NG2 glia remained (arrowheads **B2**). At P8, *Nkx2.1*-derived NG2 and Olig2 glia disappeared completely and were replaced by NG2 and Olig2 glia that did not expressed the YFP and were not derived from Nkx2.1 germinal domains (open arrowheads in **A2** and **C2**). At all postnatal ages many *Nkx2.1*-derived GABAergic interneurons found in this region were not labeled for NG2 (arrows in **B2** and **C2**).Scale bar = 675 μm in **A1, B1, C1** and **D1**; 40 μm in **A2, B2** and **C2;** 100 μm in **D2** and D3. CC, corpus callosum; CCi, cingulate cortex; LV, lateral ventricles; SEP, septum.

DOI: 10.7554/eLife.09102.006

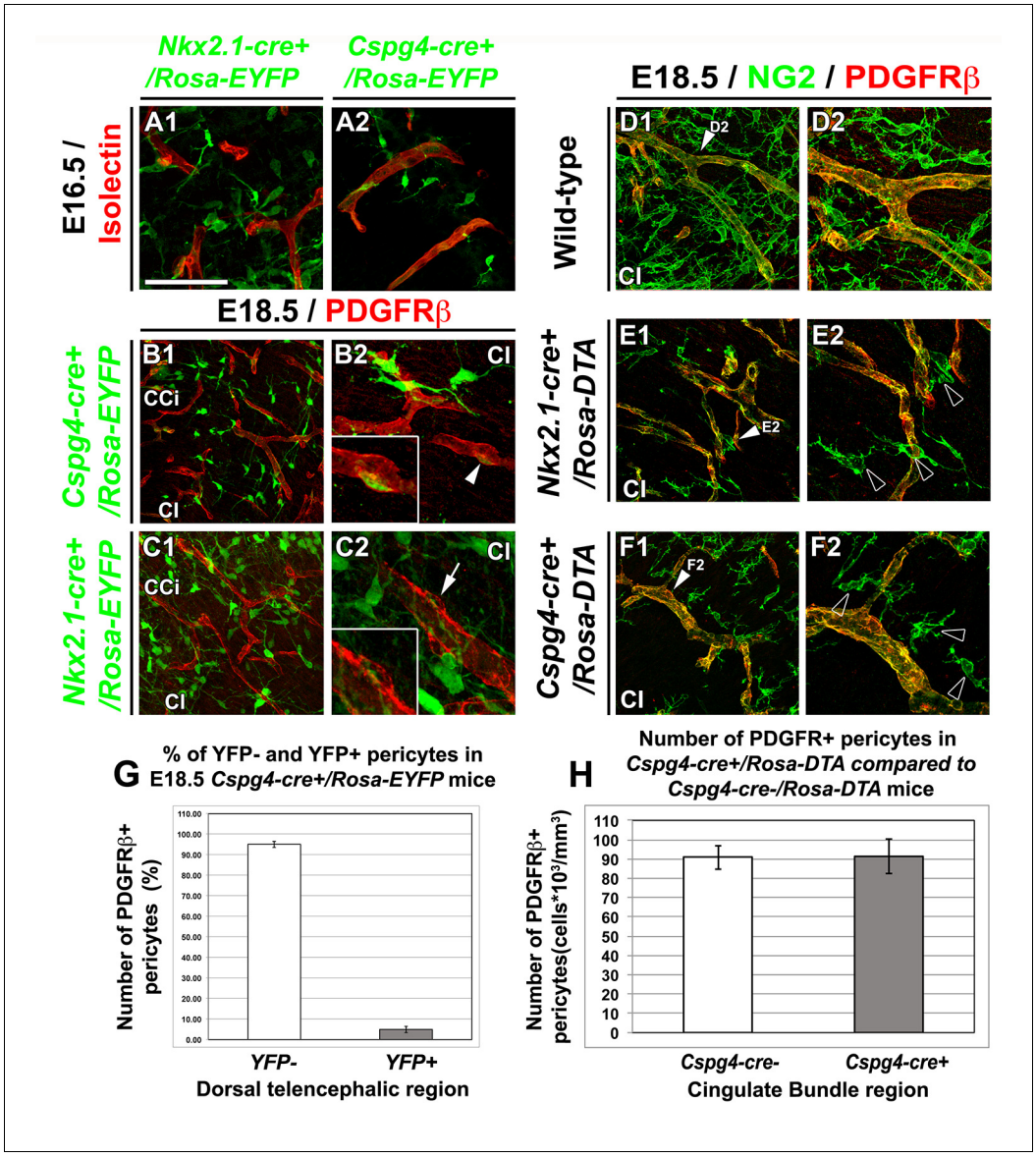

Figure 3. NG2$^+$ glia, but not pericytes, control blood vessels formation. (**A–C**) Double immunohistochemistry for the YFP and Isolectin (**A1–A2**) or PDGFRβ (**B1–B2, C1–C2**) on coronal cingulate cortex (CCi) and cingulate bundle (CI) sections of *Nkx2.1-cre$^+$/Rosa-EYFP* (**A1, C1–C2**) and *Cspg4-cre$^+$/Rosa-EYFP* (**A2, B1–B2**) mice (n=3) at E16.5 (**A1–A2**) and E18.5 (**B1–B2** and **C1–C2**). (**A–C**) From E16.5 to E18.5, numerous YFP$^+$ NG2 glia are surrounding cortical blood vessels. (**B–C**) The Cre-mediated recombination, visualized by the YFP signal, can be observed in only very few pericytes surrounding blood vessels in *Cspg4-cre$^+$/Rosa-EYFP* mice (**B2**, boxed region showing high magnification of region marked with white arrowhead), but not in *Nkx2.1-cre$^+$/Rosa-EYFP* mice (**C2,** boxed region showing high magnification of region marked with arrow). (**D–F**) Double immunohistochemistry for NG2 and PDGFRβ on coronal CI sections in wild-type (**D1–D2**), *Nkx2.1-cre$^+$/Rosa-DTA* (**E1–E2**) (n=3) and *Cspg4-cre$^+$/Rosa-DTA* (**F1–F2**) (n=3) mice at E18.5. (**D–F**) The NG2$^+$ glia form a complex cellular network around the cortico-cerebral blood vessels outlined by NG2 and PDGFRβ staining. The DTA under the control of *Nkx2.1* (**E**) and *Cspg* or *NG2* (**F**) promoters selectively depletes NG2$^+$ glia but not pericytes. **D2, E2,** and **F2** are higher power views of the cingulate region in **D1, E1,** and **F1**, respectively (white arrowheads). (**G**) Bars (means ± SEM) represent the percentage of YFP-negative and YFP-positive PDGFRβ labeled pericytes in dorsal telencephalon sections of E18.5 *Cspg4-cre$^+$/Rosa-EYFP* mice (n=10). The YFP signal in *Cspg4-cre$^+$/Rosa-EYFP* mice was not detected in PDGFRβ$^+$ embryonic pericytes of the dorsal telencephalon (95.05 ± 1.54% of pericytes are YFP-negative in the CI at E18.5, n=10). (**H**) Bars (means ± SEM; unpaired Student's *t*-test) represent the percentage of remaining PDGFRβ+ pericytes in cingulate bundle (CI) sections of E18.5 *Cspg4-cre$^+$/Rosa-DTA* mice (n=11) compared to control mice

Figure 3 continued on next page

Figure 3 continued

(n=11). No loss of PDGFRβ+ pericytes was observed in *Cspg4-cre*$^{+}$*/Rosa-DTA* mice compared to *Cspg4-cre*$^{-}$*/Rosa-DTA*. Bar = 100 μm in **B1, C1**; 50 μm in **A1, A2, D1, E1, F1**; 40 μmin **B2, C2, D2, E2, F2**.

DOI: 10.7554/eLife.09102.007

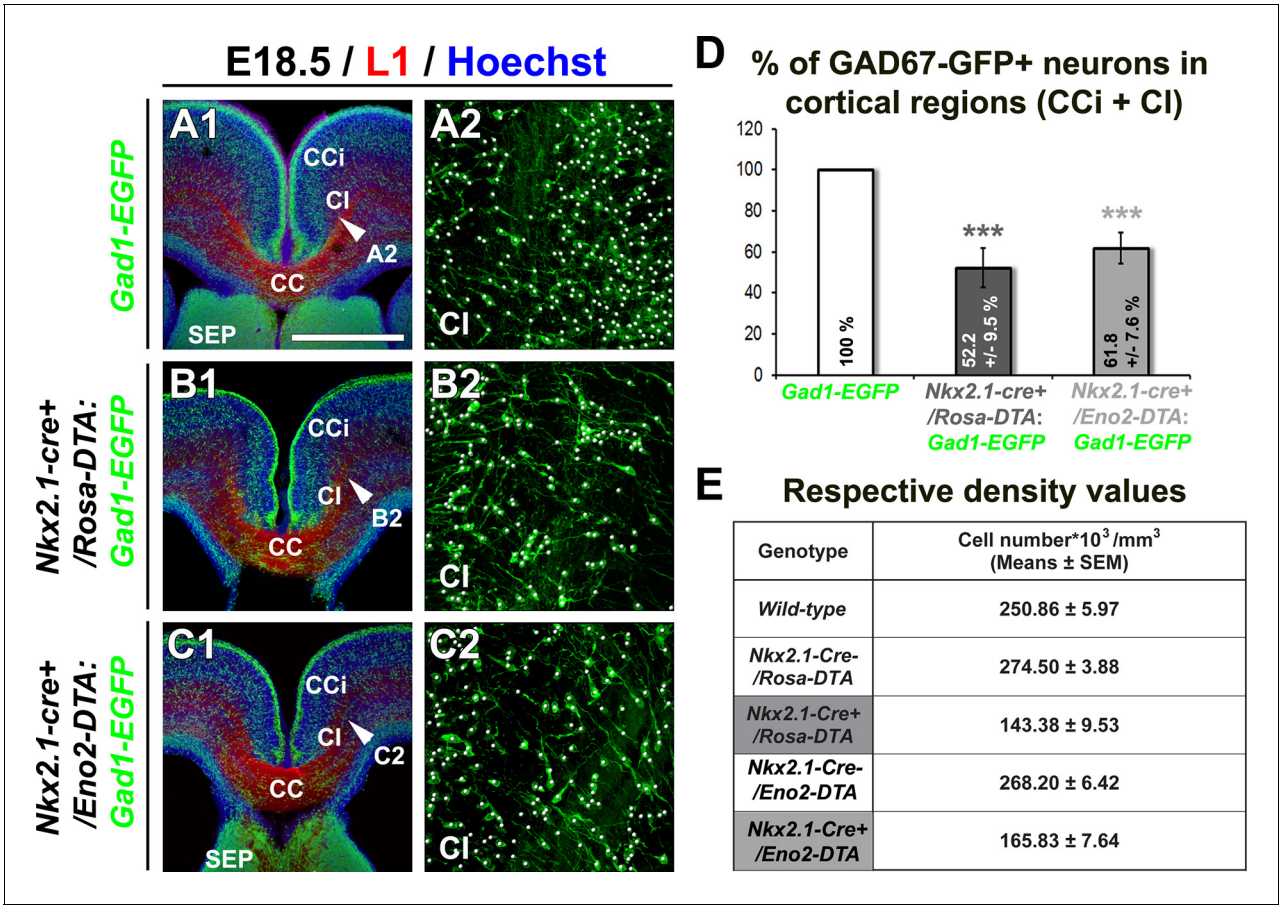

Genotype	Cell number*10^3/mm^3 (Means ± SEM)
Wild-type	250.86 ± 5.97
Nkx2.1-Cre- /Rosa-DTA	274.50 ± 3.88
Nkx2.1-Cre+ /Rosa-DTA	143.38 ± 9.53
Nkx2.1-Cre- /Eno2-DTA	268.20 ± 6.42
Nkx2.1-Cre+ /Eno2-DTA	165.83 ± 7.64

Figure 3—figure supplement 1. Drastic depletion of GAD67-GFP$^+$ neurons in *Nkx2.1$^{-/-}$*, *Nkx2.1-cre$^+$/Rosa-DTA* and *Nkx2.1-cre$^+$/Eno2-DTA* cortices. (**A–D**) Double immunohistochemistry for the GFP and L1 on coronal CI sections in *Gad1-EGFP* (n=8) (**A1–A2**), *Nkx2.1-cre$^+$/Rosa-DTA:Gad1-EGFP* (n=5) (**B1–B2**) and *Nkx2.1-cre$^+$/Eno2-DTA:Gad1-EGFP* (n= 6) (**C1–C2**) mice at E18.5. **A2, B2,** and **C2** are higher power views showing the quantification of the GAD67-GFP$^+$ interneurons (white spots) within the CI region pointed with a white arrowhead in **A1, B1,** and **C1**, respectively. (**D**) Bars (means ± SEM; unpaired Student's *t*-test) represent the percentage of remaining GAD67-GFP$^+$ interneurons in the CI of E18.5 *Nkx2.1-cre$^+$/Rosa-DTA:Gad1-EGFP* and *Nkx2.1-cre$^+$/Eno2-DTA:Gad1-EGFP* mice compared to *Gad1-EGFP* mice. Both the mutant mice exhibited equivalent loss of neurons when compared to wild-type mice. (**E**) Table of the corresponding cell density values (cell number*10^3/mm^3) (unpaired Student's *t*-test). Scale bar = 675 μm in **A1, B1,** and **C1**; 100 μm in **A2, B2,** and **C2**. CC, corpus callosum; CCi, cingulate cortex; CI, cingulate bundle; SEP, septum.

DOI: 10.7554/eLife.09102.008

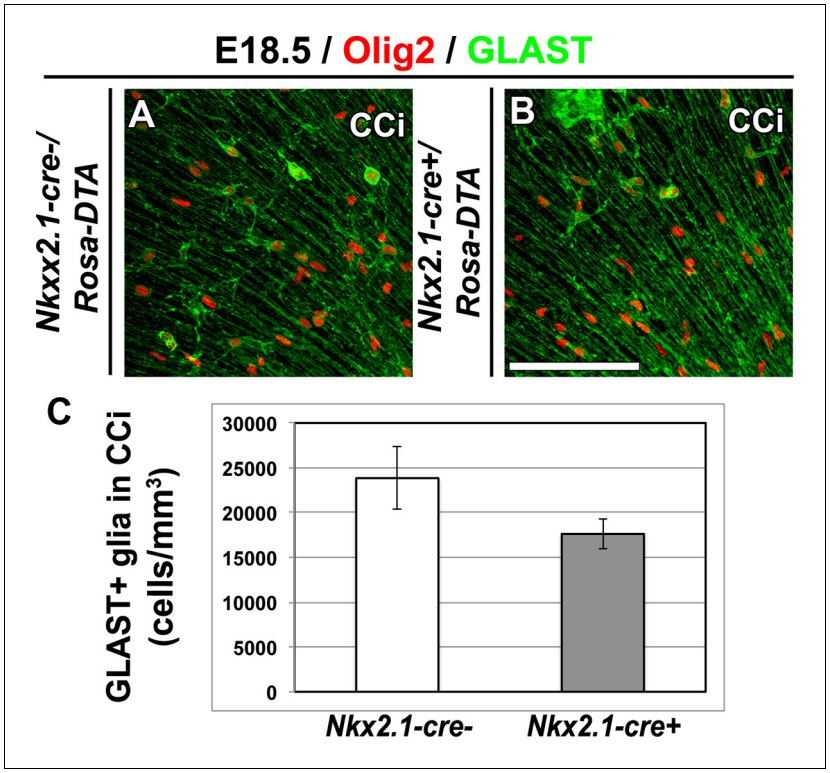

Figure 3—figure supplement 2. GLAST$^+$ astrocytes are not affected in *Nkx2.1-cre$^+$/Rosa-DTA* cingulate cortex at E18.5. (**A–B**) Double immunohistochemistry for Olig2 and GLAST in cingulate cortex (CCi) coronal sections of *Nkx2.1-cre$^-$/Rosa-DTA* mutant mice (n=4) (**A**) and *Nkx2.1-cre$^+$/Rosa-DTA* control mice (n=4) (**B**) at E18.5. Scale bar = 50 μm in **A** and **B**. (**C**) Bars (means ± SEM; unpaired Student's *t*-test) represent the density number of remaining GLAST+ astroglia in the CCi of E18.5 *Nkx2.1-cre$^+$/Rosa-DTA* mice compared to control mice. No significant loss of GLAST$^+$ astroglia was observed in *Nkx2.1-cre$^+$/Rosa-DTA* CCi compared to control mice.

DOI: 10.7554/eLife.09102.009

Figure 4. Drastic depletion of embryonic NG2$^+$ glia in *Nkx2.1-cre+/Rosa-DTA* and *Cspg4-cre+/Rosa-DTA* midline dorsal telencephalon. DAB staining for NG2 in wild-type (**A1–A3**) (n=6), *Nkx2.1-Cre$^+$/Rosa-DTA* (**B1–B3**) (n=3), *Cspg4-cre$^+$/Rosa-DTA* (**C1–C3**) (n=3), and *Nkx2.1-cre$^+$/Eno2-DTA* (**D1–D3**) (n=3) telencephalic coronal slices at E18.5. NG2$^+$ glia were completely depleted from the corpus callosum (CC), the cingulate cortex (CCi), and cingulate bundle (Cl) of *Nkx2.1-cre$^+$/Rosa-DTA* (**B1–B3**) mutant mice compared to wild-type mice (**A1–A3**). In *Cspg4-cre$^+$/Rosa-DTA* mutant mice (**C1–C3**), there was also a drastic loss of NG2$^+$ cells in medial cortical areas of the dorsal telencephalon with only few remaining cells. In *Nkx2.1-cre$^+$/Eno2-DTA* (**D1–D3**) mutant mice, there was no loss of NG2$^+$ glia in all the observed regions. **A2–A3, B2–B3, C2–C3,** and **D2–D3** are higher power views of the Cl regions in **A1, B1, C1,** and **D1,** respectively (white arrowheads). Bar = 500 μm in **A1, B1, C1,** and **D1**; 250 μm in **A2, B2, C2,** and **D2**; 125 μm in **A3, B3, C3,** and **D3**.

DOI: 10.7554/eLife.09102.010

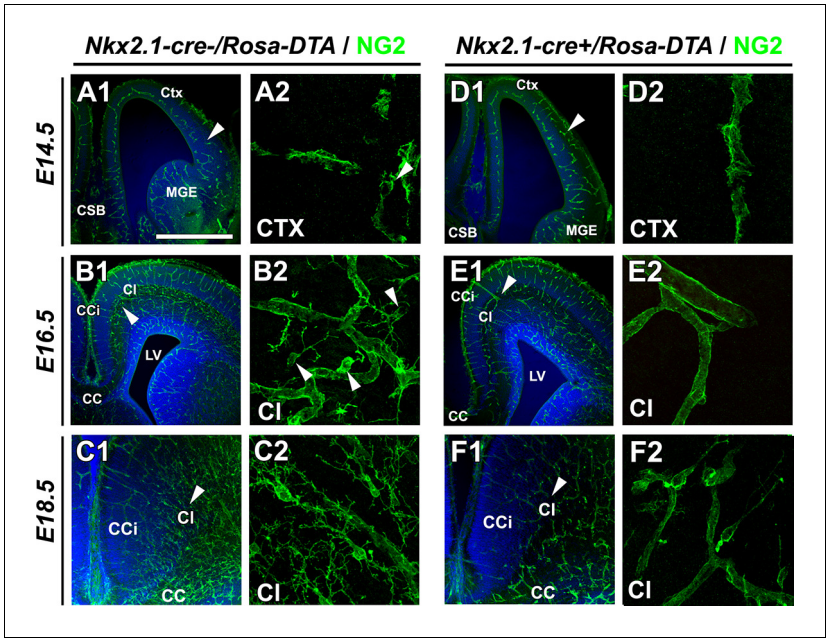

Figure 4—figure supplement 1. Drastic depletion of embryonic NG2^{+} glia in *Nkx2.1-cre^{+}/Rosa-DTA* midline dorsal telencephalon starts at E16.5. (**A–D**) Immunostaining for NG2 in *Nkx2.1-cre^{-}/Rosa-DTA* (**A1–A2** to **C1–C2**) and *Nkx2.1-cre^{+}/Rosa-DTA* (**D1**–D2 to **F1**–F2) telencephalic coronal slices at E14.5 (**A1–A2, D1–D2**), E16.5 (**B1–B2, E1–E2**) and E18.5 (**C1–C2, F1–F2**). **A2, B2, C2, D2, E2,** and **D2** are higher power views of the region in **A1, B1, C1, D1, E1,** and **F1**, respectively (white arrowheads). At E14.5, there were no significant differences in NG2^{+} glia observed in the cingulate regionof *Nkx2.1-cre^{+}/Rosa-DTA* mutant mice (n=3) compared to wild-type mice (n=3) (**A1–A2, D1–D2**). By contrast, later at E16.5, there was already a drastic loss of NG2^{+} glia populating the medio-dorsal telencephalon regionsin the *Nkx2.1-cre^{+}/Rosa-DTA* (n=3) mutant mice compared to control mice (n=3) (**B1–B2, E1–E2**). This loss was maintained at E18.5 in the *Nkx2.1-cre^{+}/Rosa-DTA* (n=3) mutant mice compared to control mice (n=3) (**C1–C2, F1–F2**). Scale bar = 675 μm in **A1, B1, C1, D1, E1,** and **F1**; 40 μmin **A2, B2, C2, D2, E2,** and **F2**.

DOI: 10.7554/eLife.09102.011

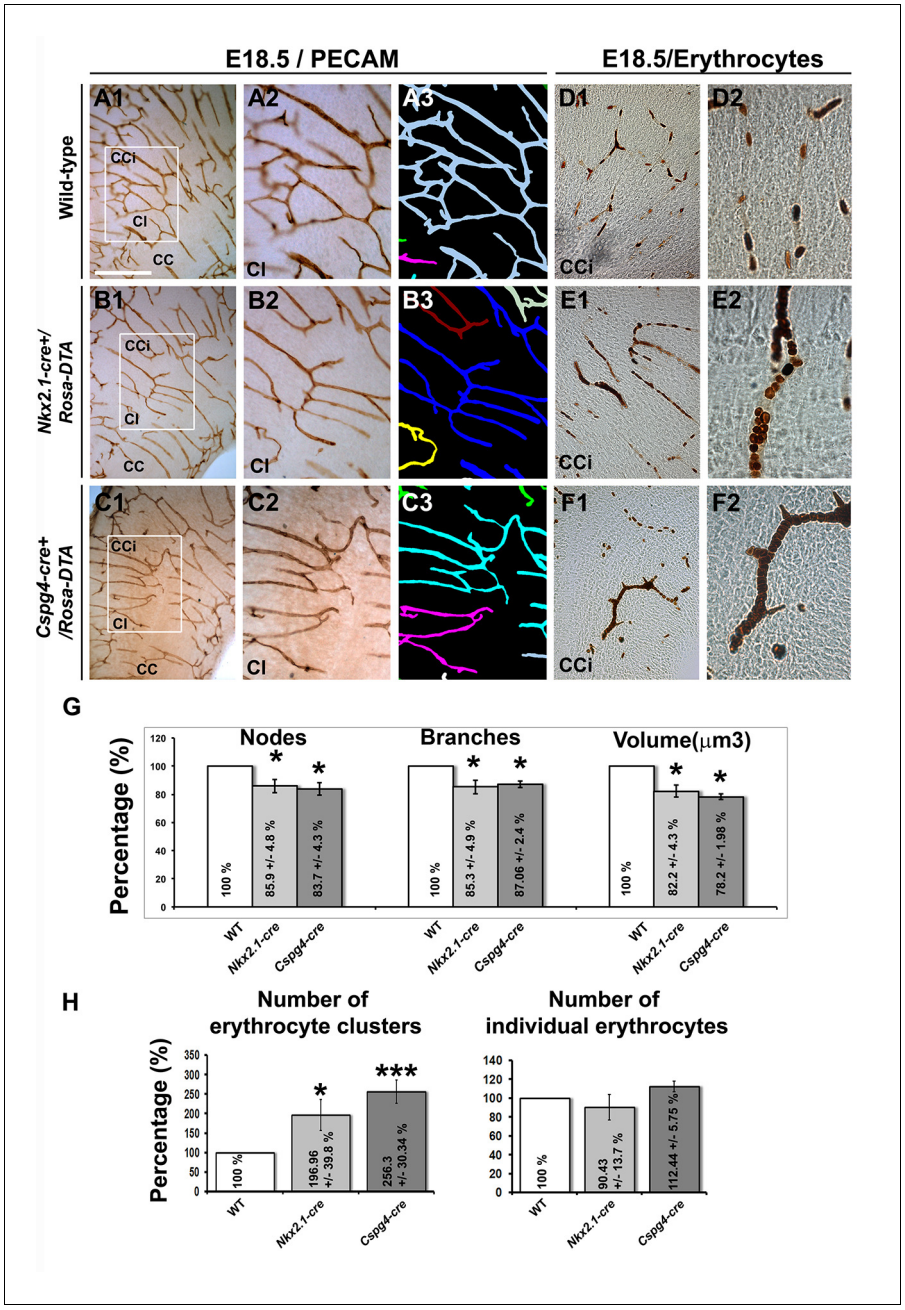

Figure 5. Blood vessel branching is similarly impaired in *Nkx2.1Cre^{+}/Rosa-DTA* and *Cspg4-cre^{+}/Rosa-DTA* mice. (**A–C**) DAB staining for PECAM and reconstitution of the vascular network using the Neurolucida tracing tool in wild-type (**A1–A3**) (n=8), *Nkx2.1-cre^{+}/Rosa-DTA* (**B1–B3**) (n=4) and *Cspg4-cre^{+}/Rosa-DTA* (**C1–C3**) (n=4) cortical coronal sections at E18.5. **A2, B2,** and **C2** are higher magnified views of the boxed regions seen in **A1, B1,** and **C1,** respectively. (**D–F**) DAB staining for erythrocytes in wild-type (**D1–D2**) (n=10), *Nkx2.1-cre^{+}/Rosa-DTA* (**E1–E2**) (n=5), and *Cspg4-cre^{+}/Rosa-DTA* (**F1–F2**) (n=5) cortical coronal sections at E18.5. (**G**) Bars (means ± SEM) represent the percentages of vessel nodes, vessel branches and volume of the vascular network in mutants compared to wild-type (n=4; unpaired Student's *t*-test). The respective absolute values per CCi section are given in ***Table 1***. All the quantified parameters were significantly decreased in mutant mice. (**H**) Bars (means ± SEM) represent the percentage of erythrocyte clusters and individual erythrocytes in mutants compared to wild-type. The respective absolute values per CCi section are given in ***Table 2*** (n=5; unpaired Student's *t*-test).The number of erythrocyte clusters showed a significant increase in all mutants. The total number of individual erythrocytes remained unchanged. Bar = **A1, B1, C1:** 250 µm; **D1, E1, F1:** 125 µm; **A2, A3, B2, B3, C2, C3:** 62.5 µm; **D2, E2, F2:** 50 µm. CCi, cingulate cortex.

DOI: 10.7554/eLife.09102.012

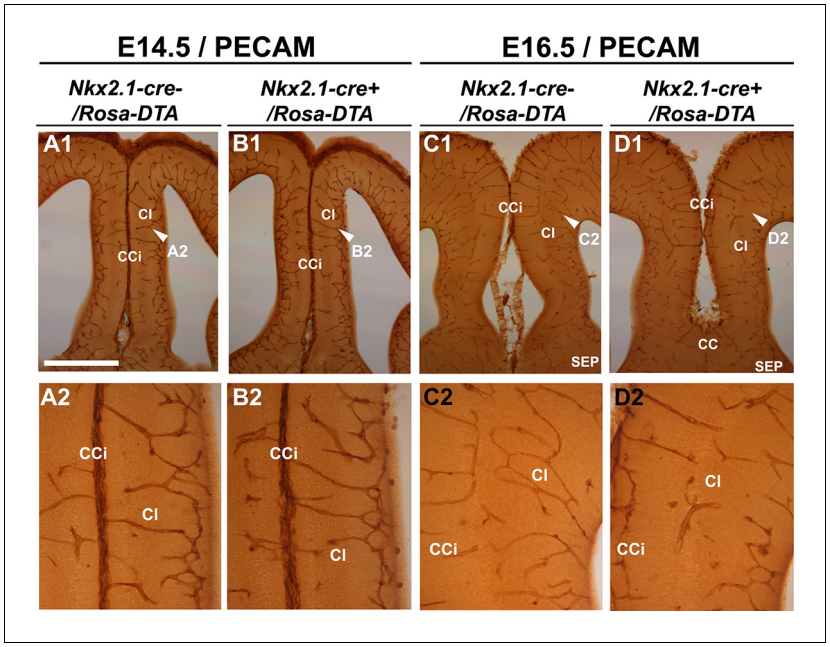

Figure 5—figure supplement 1. Embryonic *Nkx2.1*-derived NG2 glia do not control cortical blood vessels outgrowth before E16.5. (**A–D**) DAB staining for PECAM in *Nkx2.1-cre*$^{-}$*/Rosa-DTA* (n=4) (**A1-A2, C1–C2**) and *Nkx2.1-cre*$^{+}$*/Rosa-DTA* (n=4) (**B1–B2, D1–D2**) telencephalic coronal slices at E14.5 (**A1–A2, B1–B2**) and E16.5 (**C1–C2, D1–D2**). At E14.5, there was no significant blood vessel network defect observed in the cingulate region of *Nkx2.1-cre*$^{+}$*/Rosa-DTA* (**B1–B2**) mutant mice compared to wild-type mice (**A1–A2**). By contrast, later at E16.5, the blood vessel network is less developed in the *Nkx2.1-cre*$^{+}$*/Rosa-DTA* (**D1–D2**) mutant mice (**D1–D2**) compared to control mice (**C1–C2**). Scale bar = 250 μm in **A1, B1, C1,** and **D1**; 125 μm in **A2, B2, C2,** and **D2**.
DOI: 10.7554/eLife.09102.013

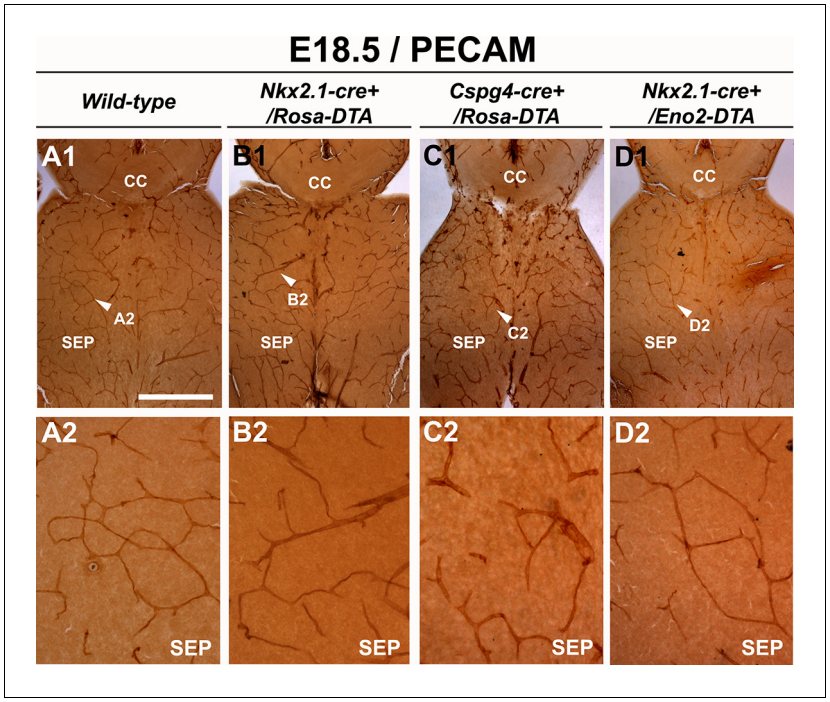

Figure 5—figure supplement 2. Blood vessel structure is impaired in the septum of *Nkx2.1-cre*$^{+}$*/Rosa-DTA* and *Cspg4-cre*$^{+}$*/Rosa-DTA* mice at E18.5. (**A–D**) DAB staining for PECAM in wild-type (n=12) (**A1–A2**), *Nkx2.1Cre*$^{+}$*/Rosa-DTA* (n=4) (**B1–B2**), *Cspg4-cre*$^{+}$*/Rosa-DTA* (n=4) (**C1–C2**) and *Nkx2.1-cre*$^{+}$*/Eno2-DTA* (n=4) (**D1–D2**) telencephalic coronal slices at E18.5. The blood vessel network was significantly impaired in the septal region (SEP) of *Nkx2.1-cre*$^{+}$*/Rosa-DTA* (**B1–B2**) and *Cspg4-cre*$^{+}$*/Rosa-DTA* (**C1–C2**) mutant mice compared to wild-type mice (**A1–A2**). In *Nkx2.1-cre*$^{+}$*/Eno2-DTA* (**D1–D2**) mutant mice, there was no significant blood vessel network defect observed in the septal region. Scale bar = 500 μm in **A1, B1, C1,** and **D1**; 125 μm in **A2, B2, C2,** and **D2**.
DOI: 10.7554/eLife.09102.014

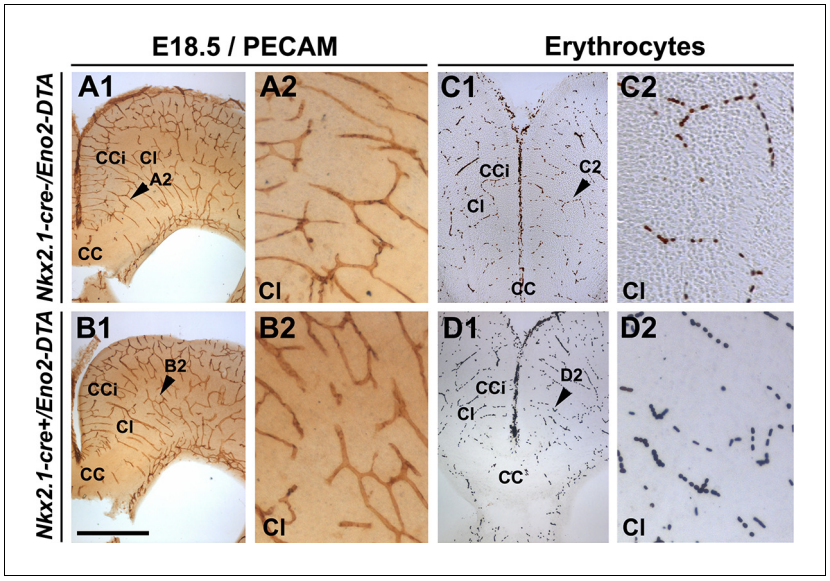

Figure 5—figure supplement 3. Embryonic *Nkx2.1*-derived GABAergic neurons do not control the development and function of cortical blood vessels. DAB staining for PECAM (**A1–A2, B1–B2**) and for erythrocytes (**C1–C2, D1–D2**) in coronal slices of the dorsal telencephalon of E18.5 wild-type (n=3) (**A1–A2, C1–C2**) and *Nkx2.1-cre*$^{+}$*/Eno2-DTA* (n=3) (**B1–B2, D1–D2**) mutant mice. (**A2, B2, C2,** and **D2**) are higher magnified views of the cingulate bundle (CI) region pointed with a black arrowhead in (**A1, B1, C1,** and **D1**), respectively. PECAM and erythrocyte staining revealed that the loss of GABAergic neurons in *Nkx2.1-cre*$^{+}$*/Eno2-DTA* mutant mice did not cause any vascular anomalies (**B2** and **D2**) compared to control mice (**A2** and **C2**). Scale bar = 500 μm in **A1, B1, C1,** and **D1**; 125 μm in **A2, B2, C2** ,and **D2**. CC, corpus callosum; CCi, cingulate cortex.

DOI: 10.7554/eLife.09102.015

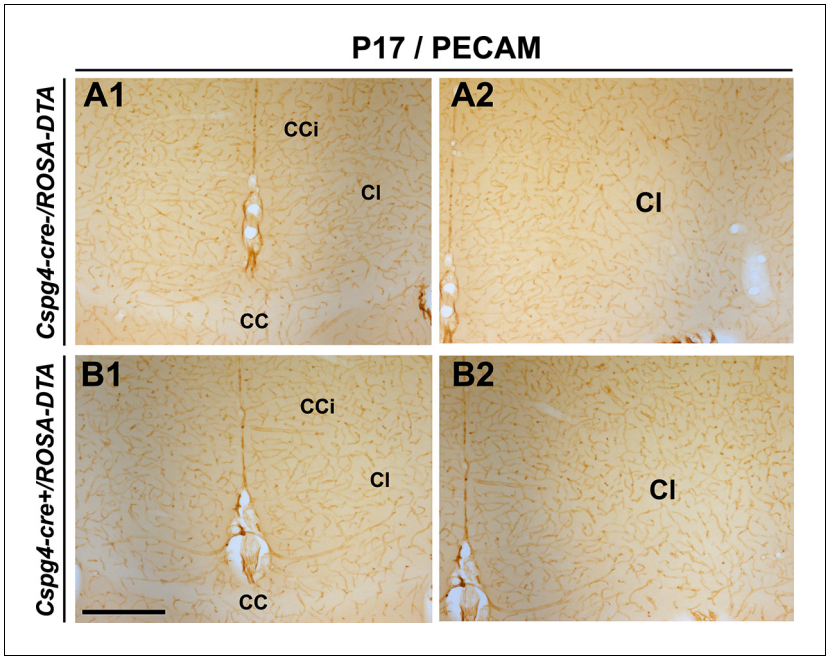

Figure 5—figure supplement 4. No significant blood vessel network defects are observed in *Cspg4-cre*$^{+}$*/Rosa-DTA* postnatal brains. (**A–D**) DAB staining for PECAM in *Cspg4-cre*$^{-}$*/Rosa-DTA* (n=3) (**A1–A2**) and *Cspg4-cre*$^{+}$*/Rosa-DTA* (n=3) (**B1–B2**) telencephalic coronal slices at P17-P19 (**A1–A2, B1–B2**). At all postnatal ages, there was no significant blood vessel network defect observed in the cingulate region and corpus callosum of *Cspg4-cre*$^{+}$*/Rosa-DTA* (**B1–B2**) mutant mice compared to control *Cspg4-cre*$^{-}$*/Rosa-DTA* (**A1–A2**) mice. Scale bar = 500 μm in **A1–A2** and **B1–B2**.

DOI: 10.7554/eLife.09102.016

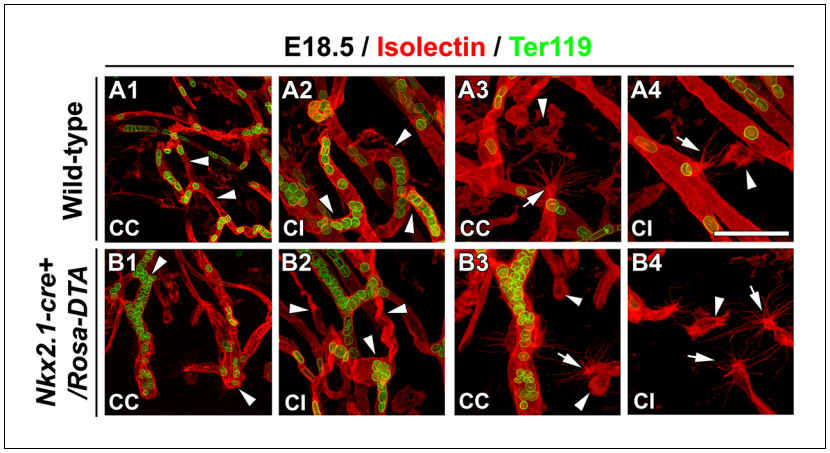

Figure 6. Macrophages and tip cells are not affected in *Nkx2*-1Cre^{+}/Rosa-DTA mice. (**A–B**) Double immunohistochemistry for Isolectin and Ter119, to visualize erythrocytes, on 250-μm-thick coronal of corpus callosum (CC) and cingulate bundle (CI) sections in wild-type (**A1–A4**) (n=5) and *Nkx2.1-cre*$^{+}$*/Rosa-DTA* (**B1–B4**) (n=5) mice at E18.5. In the CC and the CI (**B1–B2**) of *Nkx2.1-cre*$^{+}$*/Rosa-DTA* mice, the blood vessels have a twisted shape and the erythrocytes are clustered (white arrowheads in **B1** and **B2**) compared to the wild-type vessels that formed a regular network (white arrowheads in **A1** and **A2**). In the CC and the CI of both wild-type (**A3–A4**) and *Nkx2.1-cre*$^{+}$*/Rosa-DTA* mice (**B3–B4**), guidepost macrophages labeled by the isolectin (white arrowheads in **A3–A4** and **B3–B4**) are found in the close vicinity of the tip cells (white arrows in **A3–A4** and **B3–B4**). The tip cells exhibit the same morphology and the same number of filopodia with similar length in both circumstances. Bar = 60 μm in **A1, B1**; 40 μm in **A2, B2, A3, A4, B3, B4**.

DOI: 10.7554/eLife.09102.017